Available online at www.sciencedirect.com
SCIENCE DIRECT®
Tectonophysics 378 (2004) 241–262
TECTONOPHYSICS
www.elsevier.com/locate/tecto

Physical interpretation of the breakdown process using a rate- and state-dependent friction law

M. Cocco*, A. Bizzarri, E. Tinti

Department of Seismology and Tectonophysics, Istituto Nazionale di Geofisica e Vulcanologia Roma, Via di Vigna Murata 605, Rome 00143, Italy

Accepted 11 September 2003

Abstract

We study the dynamic traction and the slip velocity evolution within the cohesive zone during the propagation of a dynamic rupture using rate- and state-dependent constitutive laws. We solve the elastodynamic equation for a 2-D in-plane crack using a finite difference algorithm. We show that rate and state constitutive laws allow a quantitative description of the dynamic rupture growth. We confirm the findings of previous studies that slip weakening (SW) is a characteristic behavior of rate and state friction. Our simulations show that the state variable evolution controls the slip acceleration and the slip-weakening behavior. These modeling results help in understanding the physical interpretation of the breakdown process and the weakening mechanisms. We compare the time histories of slip velocity, state variable and total dynamic traction to investigate the temporal evolution of slip acceleration and stress drop during the breakdown time. Because the adopted analytical expression for the state variable evolution controls the slip velocity time histories, we test different evolution laws to investigate slip duration and the healing mechanisms. We show that the classic slowness or slip laws do not yield fast restrengthening or self-healing, although they appropriately describe rupture initiation, propagation and the long-term restrengthening during the interseismic period. Self-healing rupture mode, yielding to short slip durations, has been obtained for homogeneous faults by modifying the evolution law introducing a fast restrengthening of dynamic traction immediately after the weakening phase. In this study, we discuss how the direct effect of friction and the friction behavior at high slip rates affect the weakening and healing mechanisms.

Keywords: Fault friction; Earthquake rupture; Rate- and state-dependent constitutive laws; Cohesive zone; Slip weakening; Fracture energy

1. Introduction

The modeling of earthquake nucleation and the subsequent dynamic propagation requires using a fault constitutive law that controls the traction evolution and the slip acceleration and allows the absorption of a finite fracture energy at the crack tip. One of the most widely used constitutive equations is the slip weakening (SW) law, which consists in assuming that friction (i.e., total dynamic traction) is a function of slip only (Barenblatt, 1959; Ida, 1972; Palmer and Rice, 1973; Andrews, 1976a,b; Ohnaka and Yamashita, 1989). It involves a finite fracture energy and prescribes the traction evolution within the cohesive zone (see Cocco and Bizzarri, 2002, and references therein). The adoption of a SW law is useful to calculate synthetic ground

* Corresponding author. Tel.: +39-06-518-60401; fax: +39-06-518-60507.
E-mail address: cocco@ingv.it (M. Cocco).

0040-1951/$ - see front matter © 2003 Elsevier B.V. All rights reserved.
doi:10.1016/j.tecto.2003.09.015

motions with dynamic models (see Aochi and Fukuyama, 2002). An alternative constitutive formulation, represented by the rate- and state-dependent (R&S) laws, considers that friction depends on slip velocity and state variable (Dieterich, 1979, 1986, 1992, 1994; Ruina, 1980, 1983; Scholz, 2002; Marone, 1998 and references therein). This class of constitutive relations includes an evolution law for the state variable that involves a friction dependence on time. These two constitutive formulations are alternative only for the description of the nucleation process (see Dieterich, 1992; Ohnaka and Shen, 1999), but they provide a very similar description of the dynamic crack propagation (see Okubo, 1989; Bizzarri et al., 2001). In the following of the paper, we refer to the cohesive zone (or breakdown zone) as the zone of shear stress degradation near the tip of a propagating dynamic rupture front. The breakdown processes are those phenomena occurring within the cohesive zone responsible for the fracture energy absorption and the slip acceleration. We emphasize that rate and state constitutive laws allow a quantitative description of the dynamic rupture growth, as shown for instance by Bizzarri et al. (2001).

In this paper, we aim to study the dynamic traction and the slip velocity evolution within the cohesive zone (see Fig. 1) using a R&S constitutive law to understand the physical processes controlling the weakening and the healing mechanisms (i.e., the slip duration during the dynamic rupture propagation). We start noting that the SW behavior is the result of the dynamic failure process: In order to have a finite stress release the total dynamic traction drops when slip increases, which results in the commonly used slip-weakening behavior. This process occurs at the crack tip in a finite extended zone named the cohesive zone (Ida, 1972; Andrews, 1976a,b; Ohnaka, 1996). Therefore, slip weakening must occur within the cohesive zone, but this behavior is the result of the

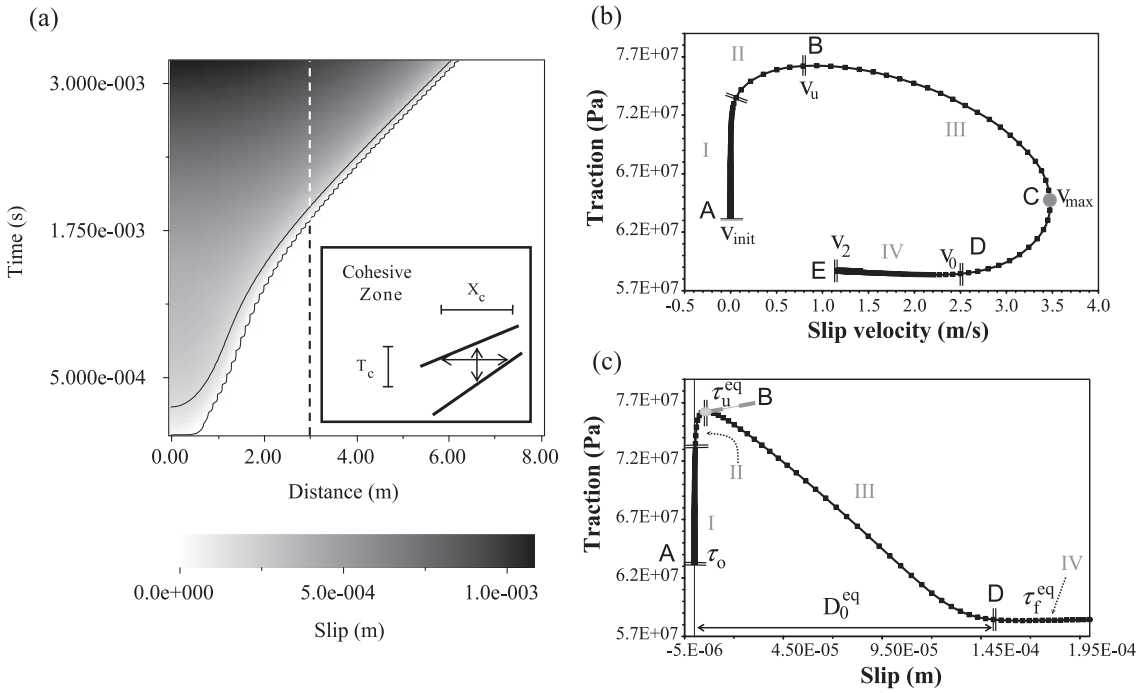

Fig. 1. (a) Spatio-temporal evolution of slip for a 2-D in-plane crack obeying to a slowness constitutive law (Eq. (1)). Slip amplitudes are shown with the grey scale. The black lines depict the cohesive zone where the total dynamic traction drops from the maximum yield stress (τ_u^{eq}) to the kinetic friction (τ_f^{eq}). The box inserted in panel (a) depicts a zoom of the cohesive zone: T_c is the duration and X_c is the spatial extension of the cohesive zone. Phase diagram (i.e., traction vs. slip rate) (b) and traction behavior versus slip (c) are shown for the propagating rupture at the fault point $x_1 = 3.0$ m. We indicate different stages of the dynamic rupture with roman numbers (I–IV) as well as with letters (A–E) in both panels. Initial and constitutive parameters used for these calculations are listed in Table 1; τ_0 is the initial stress.

physical processes controlling the breakdown zone. Therefore, the intriguing question is what controls the traction evolution and the weakening mechanisms that allow the slip to accelerate and to heal. It is well known from the literature that slip-weakening is a characteristic feature of rate and state constitutive laws (Okubo and Dieterich, 1984; Guatteri et al., 2001; Bizzarri et al., 2001). Okubo (1989) and Cocco and Bizzarri (2002) have demonstrated that the critical slip weakening distance (D_0) is different from the parameter L of the R&S formulation. Bizzarri and Cocco (2003) have discussed the relation between these two length-scale parameters both analytically and numerically and they have proposed a scaling law relating D_0 and L. They also emphasized an intrinsic limitation, which is characteristic of R&S models, to prescribe "a priori" the traction evolution within the cohesive zone, which depends on "unknown" slip velocity values associated with particular stages of the breakdown process.

In the present study, we will use rate- and state-dependent constitutive laws to model the temporal evolution of slip velocity and dynamic traction during the propagation of a 2-D in-plane crack. The goal is to understand the frictional control of slip weakening behavior and rupture healing. In the literature many different studies have discussed numerical simulations of dynamic slip on homogeneous faults showing either crack-like rupture mode or self-healing pulse propagation (Cochard and Madariaga, 1994, 1996; Perrin et al., 1995; Beeler and Tullis, 1996; Zheng and Rice, 1998). The healing of slip, leading to short slip durations or self-healing pulse propagation mode, has been related either to stress and/or strength (frictional) heterogeneity (see for instance Beroza and Mikumo, 1996; Bizzarri et al., 2001). Self-healing ruptures have also been shown to appear in rupture propagation between dissimilar materials (Weertman, 1980; Andrews and Ben-Zion, 1997; Cochard and Rice, 2000). In this study, we focus on the rupture propagation along homogeneous faults. In such a homogeneous configuration, healing mechanism and self-healing pulses are related to the friction law (Perrin et al., 1995; Cochard and Madariaga, 1996; Beeler and Tullis, 1996; Zheng and Rice, 1998). We review and discuss previous modeling results and interpret the physical mechanisms controlling the breakdown process and the slip acceleration in the framework of a rate and state constitutive formulation.

2. Methodology

In this study, we solve the elastodynamic equation for a 2-D in-plane shear crack for which the displacement and the shear traction depend on time and on only one spatial coordinate. We assume that the crack propagates only in the x_1-direction. The medium is supposed to be infinite, homogeneous and elastic everywhere except along the fracture line. We solve the equation of motion by using a finite difference (FD) approach described in Andrews (1973) and Andrews and Ben-Zion (1997). Bizzarri et al. (2001) describe the details of the numerical solution. We can use in our procedure either R&S laws with slowness (ageing) evolution equation (Dieterich, 1986):

$$\tau = \left[\mu_* - a\ln\left(\frac{V_*}{V}+1\right) + b\ln\left(\frac{\Phi V_*}{L}+1\right)\right]\sigma_n^{\mathrm{eff}}$$
$$\frac{\mathrm{d}}{\mathrm{d}t}\Phi = 1 - \frac{\Phi V}{L} \tag{1}$$

or with slip evolution equation (Beeler et al., 1994),

$$\tau = \left[\mu_* + a\ln\left(\frac{V}{V_*}\right) + b\ln\left(\frac{\Theta V_*}{L}\right)\right]\sigma_n^{\mathrm{eff}}$$
$$\frac{\mathrm{d}\Theta}{\mathrm{d}t} = -\frac{\Theta V}{L}\ln\left(\frac{\Theta V}{L}\right) \tag{2}$$

We can also use a slip weakening law as introduced by Andrews (1976a,b):

$$\tau = \begin{cases} \tau_{\mathrm{u}} - (\tau_{\mathrm{u}} - \tau_{\mathrm{f}})\dfrac{u}{D_0} & u < D_0 \\ \tau_{\mathrm{f}} & u \geq D_0 \end{cases} \tag{3}$$

In Eqs. (1) and (2), V is the slip velocity, Φ and Θ are the state variables, μ_* and V_* are arbitrary reference values for the friction coefficient and for the slip velocity, respectively; a, b and L are the three constitutive parameters. In general, in this formulation the state variable has the physical meaning of an average contact time of asperities between the sliding surfaces (Dieterich, 1986; Ruina, 1983). The first equation in Eqs. (1) and (2) is usually named in the literature the

governing equation, while the second is called the evolution equation. The evolution law in Eq. (1) is the slowness law (Ruina, 1983; Beeler et al., 1994; Roy and Marone, 1996), and it includes true ageing, while the one in Eq. (2) is usually named the slip law. In this work we only consider a velocity weakening regime (that is, $b>a$). In Eq. (3), τ_u is the upper yield stress, τ_f is the final kinetic friction level, u is the slip and D_0 is the characteristic slip-weakening distance.

The characteristic length scale parameters of these two constitutive formulations are the slip weakening distance D_0 and the parameter L: the former represents the slip required for traction to drop, the latter is the characteristic length for the renewal of a population of contacts along the sliding surface and controls the evolution of the state variable. In two recent papers Cocco and Bizzarri (2002) and Bizzarri and Cocco (2003) have investigated the slip-weakening behavior of the rate- and state-dependent constitutive law (Eq. (1)) and have shown that these two length scale parameters are different. They propose a scaling law between D_0 and L, which states that their ratio is nearly 15 (in agreement with Okubo, 1989; Guatteri and Spudich, 2000) and found analytical relations to associate SW and R&S constitutive parameters. We further discuss these results in the present study with the perspective to provide a physical interpretation of the breakdown processes.

3. Slip weakening and breakdown process in the R&S formulation

We discuss in this section the evolution of the dynamic traction during the breakdown process and the consequent SW behavior. We start by summarizing the results of previous work and we therefore focus on the physical interpretation of the breakdown process in the framework of R&S dependent laws. Bizzarri et al. (2001) have clearly shown that rate- and state-dependent friction laws can provide a quantitative description of the rupture growth and dynamic propagation. We show in Fig. 1 the results of a numerical simulation performed with our 2-D finite difference code for an in-plane rupture governed by R&S friction adopting a slowness evolution law (Eq. (1)) for a reference set of parameters listed in Table 1. These calculations have been performed using values typical of laboratory experiments: the medium surrounding the crack is linear elastic, homogeneous, Poissonian and the total fault length is equal to 20 m. After initiation, the crack propagates symmetrically with respect to $x_1=0$. At the initial stage the fault is at steady state, except in the nucleation region, which is 3 m wide. The nucleation strategy adopted for the simulations is a time weakening controlled by the state variable and it is described in Bizzarri et al. (2001). Fig. 1 shows the spatio-temporal evolution of slip (a) for a homogeneous fault where the spatial discretization is $\Delta x=0.01$ m, and Δt is fixed from the Courant–Friedrichs–Levy ratio w_{CFL}, defined as $\beta \Delta t/\Delta x$. This figure is useful to depict the cohesive zone, its dimension and duration during the crack propagation. The dependence of total dynamic traction on slip velocity and slip is shown in (b) and (c), respectively. The convergence and stability of numerical simulations are discussed in detail in Bizzarri and Cocco (2003). Fig. 1c illustrates that, adopting a R&S friction law, the dynamic traction clearly shows the characteristic slip-weakening behavior (in agreement with Okubo, 1989; Dieterich and Kilgore, 1994 among various others). According to Cocco and Bizzarri (2002) we call the slip required for traction to drop as "equivalent" slip weakening distance D_0^{eq}

Table 1

Elastic moduli (Lamé constants)	$\lambda=G=27$ GPa
P and S wave velocities	$\alpha=5196$ m/s, $\beta=3000$ m/s
Effective normal stress	$\sigma_n^{eff}=100$ MPa
R&S constitutive parameters	$a=0.012$, $b=0.016$, $L=1\times10^{-5}$ m
Reference value for the friction coefficient	$\mu_*=0.56$, $V_*=1000$ m/s
Initial values of the state variable within the nucleation zone and outside	$\Phi(x_1,t=0)=\begin{cases}\Phi_{nucl}=1\times10^{-4}\text{ s}, & x_1\in[-1.5\text{ m},1.5\text{ m}]\\ \Phi^{ss}(v_{init}), & \text{elsewhere}\end{cases}$
Fault discretization: spatial and temporal time steps	$\Delta x=0.01$ m, $w_{CFL}=\beta\Delta t/\Delta x$

which does not coincide with the characteristic length scale parameter (L) of the R&S formulation (see also Gu, 1984; Gu and Wong, 1991; Nakatani, 2001).

In Fig. 2, we compare the time histories of total traction, slip, slip velocity and state variable, normalized in amplitude and calculated for the same model parameters used in Fig. 1 in the same fault position ($x_1 = 3.0$ m, i.e., outside the nucleation region). We have subdivided the time window shown in Fig. 2 in five distinct stages, which comprise the duration of the whole breakdown process, and that are associated with particular values of the slip velocity in Fig. 1b. Fig. 3 shows the 3-D plots of the relevant physical parameters: (a) and (b) illustrate the total dynamic traction as a function of state variable and slip or slip velocity, respectively; (c) shows the state variable as a function of slip and slip velocity. These figures highlight several important conclusions. First, the state variable evolution drives the slip acceleration and the traction drop during the weakening phase. This is evident in Figs. 2 and 3c: the state variable evolves from its initial to the new steady state value during phase II and the beginning of phase III. The slip velocity reaches its peak when the state variable has already reached the final steady-state value (see Figs. 2 and 3b,c). The traction increase during phase II is associated with this evolution. We emphasize that the traction does not reach its maximum simultaneously with to the peak of the slip velocity. Slip weakening (phase III) begins when the state variable is evolving in a very short time and is half-way from the final value (Figs. 2 and 3a). Moreover, the slip velocity evolution shows a clear

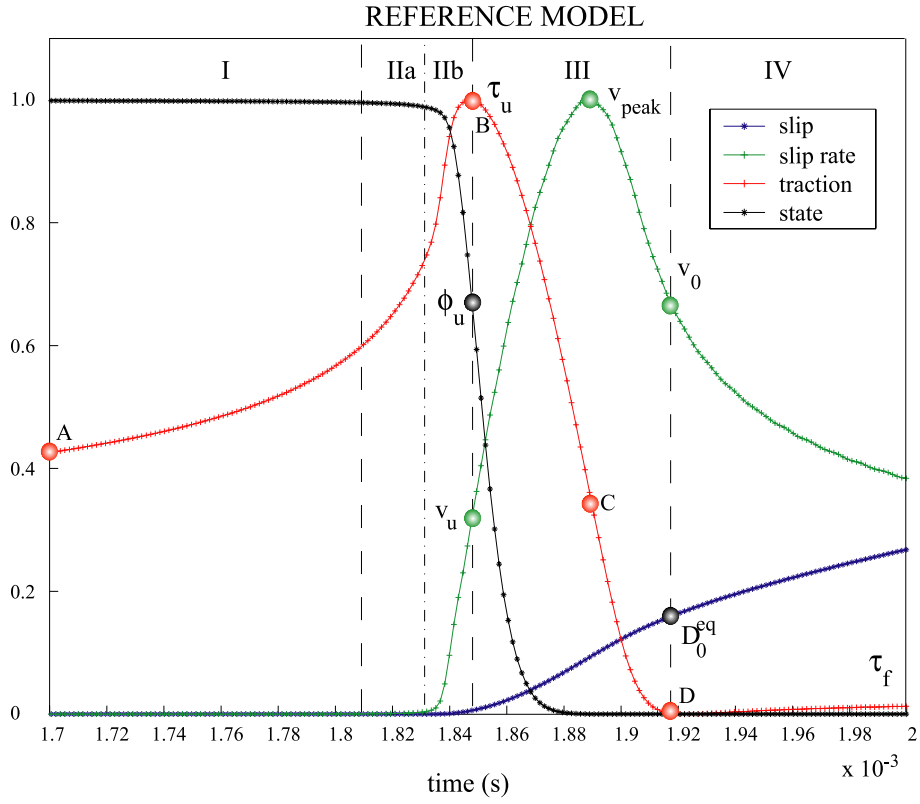

Fig. 2. Time histories of slip, slip velocity, state variable and total dynamic traction for the simulation shown in Fig. 1 calculated at the same fault position. The amplitudes of each time history are normalized to its peak value to allow the comparison. The amplitude of peak slip velocity for this simulation is 2.65 m/s (at 1.89×10^{-3} s), while peak value of traction is 7.62×10^7 Pa occurring at 1.85×10^{-3} s. The residual stress amplitude at 1.92×10^{-3} s is equal to 5.85×10^7 Pa. The value of the equivalent slip weakening distance is 1.6×10^{-4} m. The different stages of the dynamic failure process illustrated in Fig. 1 are reproduced here for comparison. The slip velocity values at particular stage of the breakdown process are indicated and they are associated to the values of the other physical quantities.

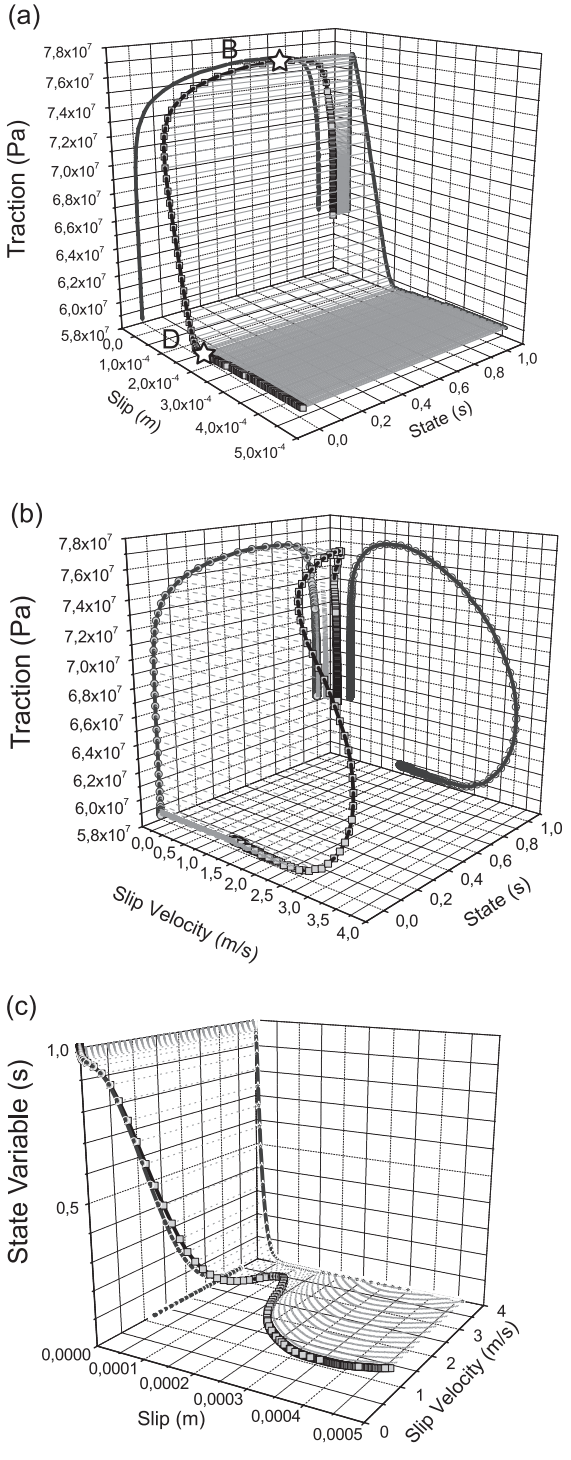

velocity hardening behavior (phase I and II, from A to B in Fig. 1b) followed by a velocity weakening (B to C in Fig. 1b, belonging to phase III). Therefore, we can conclude that slip weakening and velocity weakening occur simultaneously and they are both driven by the state variable evolution (quite clear in Fig. 3). Once slip velocity has reached its peak value (C in Fig. 1b), the traction further decreases while slip decelerates (C to D in Fig. 1b). The slip velocity evolution between the points C and D still belongs to phase III (i.e., slip weakening see Fig. 2). The fact that point C does not coincide with D means that peak slip velocity occurs before the stress is at the kinetic level and the slip is equal to D_0^{eq}.

Fig. 4 shows different slip weakening curves computed with different values of the parameter L and leaving unchanged all the other constitutive and initial parameters. This figure shows that the equivalent slip weakening distance is larger than the parameter L (see Cocco and Bizzarri, 2002) and that the absorbed fracture energy, as well as the resulting weakening rate, depend on the value adopted for the parameter L. Bizzarri and Cocco (2003) have proposed the following analytical relations to associate SW parameters to R&S constitutive and initial ones. Here we summarize these equations starting by the analytical relation between the two length-scale parameters:

$$D_0^{eq} = L\ln\left(\frac{V_0}{V_{init}}\right) \cong \frac{(\tau_u^{eq} - \tau_f^{eq})}{b\sigma_n} L. \quad (4)$$

This equation shows that the proportionality factor relating D_0^{eq} and L depends on the initial velocity (V_{init}) and on the slip velocity (V_0) reached when the slip is equal to D_0^{eq} (see Fig. 2). The latter is unknown a priori. The last term in Eq. (4) expresses an approximate relation where the proportionality factor scales with the stress drop. This relation is valid only for the slowness law (Eq. (1)), as it will be discussed in the following. The dependence on L is well

Fig. 3. 3-D phase trajectories illustrating total dynamic traction as a function of slip and state (a) or slip velocity and state (b). (c) shows the state variable as a function of slip and slip velocity. The state evolves from the initial steady state (L/V_{init}) up to the final, new steady state (L/V_0). These calculations have been performed with the same constitutive parameters and at the same fault position as in previous figures. Letters B and D depict the same points as in previous figures.

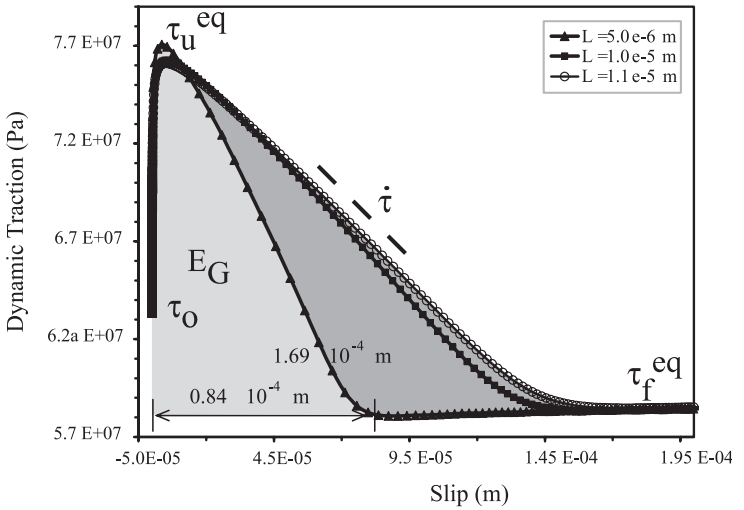

Fig. 4. SW curves calculated from different simulations having the same initial and constitutive parameters (the same used in previous figures and listed in Table 1) except the characteristic length L, ranging between 5 and 11 μm. We only change the spatial discretization to resolve appropriately the size and duration of the cohesive zone ($\Delta x = 0.005$ m). The shaded areas indicate the fracture energy, E_G, for two distinct configurations with the smallest and largest adopted L value. The equivalent slip weakening distance is 84 μm for $L = 5$ μm, 152 μm for $L = 10$ μm and 169 μm for $L = 11$ μm.

represented by Eq. (4) but the dependence on a and b is much more complex since both the yield stress and the kinetic friction depend on the constitutive parameters. In fact, numerical simulations presented by Bizzarri and Cocco (2003) have shown that the kinetic friction depends on the difference $(b - a)$ as:

$$\tau_f^{eq} = \left[\mu_* + (b-a)\ln\left(\frac{V_*}{V_0}\right)\right]\sigma_n^{eff}. \quad (5)$$

The yield stress is related to the constitutive parameters through values (unknown a priori) of slip velocity (V_u) and state variable (Φ_u) reached when total traction is at the peak value (see Fig. 2). For the slowness law (Eq. (1)) the yield stress can be expressed as:

$$\tau_u^{eq} = \left[\mu_* + a\ln\left(\frac{V_u}{V_*}\right) + b\ln\left(\frac{\Phi_u V_*}{L}\right)\right]\sigma_n^{eff} \quad (6)$$

Eqs. (4), (5) and (6) allow the association of R&S and SW constitutive parameters. They also summarize the dependence of yield stress, kinetic friction and equivalent slip weakening distance on the R&S constitutive parameters. Fig. 4 clearly shows that both the kinetic friction level and the yield stress do not depend on the value adopted for the parameter L, which indeed controls the equivalent slip weakening distance as stated in Eq. (4). Consequently, the fracture energy and the weakening rate depend on the parameter L. Numerical simulations, performed with constitutive parameters and fault parameterization at the laboratory scale, yield fracture energy values ranging between 10^3 and 10^4 J/m^2, in agreement with previous studies (Okubo and Dieterich, 1984). Recent studies have attempted to estimate the critical slip weakening distance from strong motion recordings (Ide and Takeo, 1997; Guatteri and Spudich, 2000) and suggested quite large values up to 0.5 m. There are several concerns, however, about the reliability of such large values of the critical slip weakening distance. Guatteri and Spudich (2000) pointed out that there is a limitation to infer D_0 from ground motion waveforms because of the trade-off between critical slip and strength excess (i.e., the difference between yield and initial stress values). If the slip weakening law is assumed as the constitutive relation and D_0 is the characteristic length scale parameter of the dynamic problem, then the nucleation patch scales with D_0. Cocco and Bizzarri (2002) have emphasized that in this case, adopting values of the critical slip weakening distance ranging between 0.1 and 1 m, the nucleation patch dimension would be a large fraction of the whole rupture area. On

the contrary, in the framework of a rate and state formulation, the nucleation patch scales with L and not with D_0^{eq} (if L were 1 mm the nucleation patch would be less than 1 km, see also Lapusta and Rice, 2003). However, in order to use the results of numerical simulations discussed here and to use the analytical relations proposed by Bizzarri and Cocco (2003) we have to solve the problem of scaling these results from the laboratory scale to the actual fault dimensions. Cocco and Bizzarri (2002) suggest that, if this scaling is allowed, according to laboratory experiments (Marone and Kilgore, 1993; Mair and Marone, 1999) L can be as large as 1 cm and the proposed scaling law would yield D_0 value close to 0.2 m. In this case, the fracture energy ranges between 10^6 and 10^7 J/m^2. However, the scaling of constitutive parameters from laboratory to actual fault dimensions is still under debate and alternative explanations exist, as we will discuss in the following.

4. The evolution law and the dynamic rupture growth

In the previous section we have discussed the results of several simulations performed for a 2-D in-plane crack obeying to a rate- and state-dependent law and using a slowness evolution equation as defined in Eq. (1). We have demonstrated that SW occurs within the breakdown zone and that the critical slip weakening distance is larger than the characteristic length scale parameter of the R&S formulation. We have concluded that the state variable evolution controls the weakening process and the consequent slip acceleration. Therefore, it is likely to expect that the analytical relation used for the evolution law can affect the SW behavior and the absorbed fracture energy. To test this finding, we have compared the SW curves resulting from numerical simulations performed by using the same constitutive and initial parameters for a slowness and a slip evolution laws, defined in Eqs. (1) and (2), respectively. Fig. 5 shows this comparison: Our simulations clearly show that the slip weakening curves resulting from these two evolution laws are very different and that the equivalent slip weakening distance for a slip law is much lower than that obtained for a slowness law (Bizzarri and Cocco, 2003). This result corroborates the idea that the state variable controls the weakening process, and it suggests that the analytical relation (Eq. (4)), which was established for the slowness law, is not valid for the slip law. The kinetic friction is the same because the steady state friction value is the same for the two laws and the yield stress does not substantially change with the evolution law.

We have also shown in previous calculations that the state variable evolution controls the time evolution of slip and therefore it should control the healing of slip. Several authors in fact suggested that the evolution law controls the healing mechanisms and the

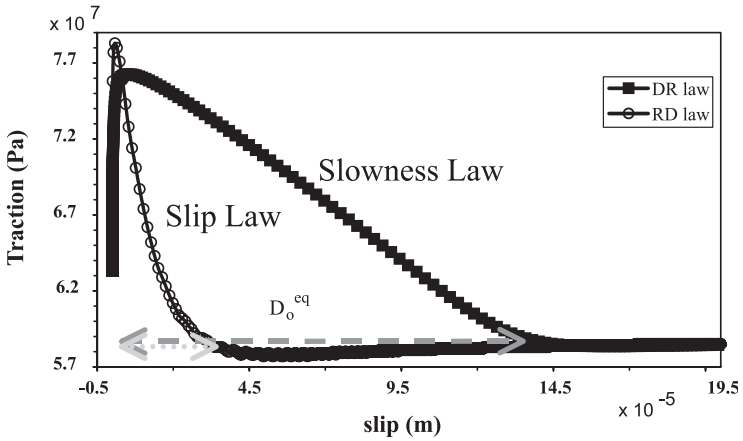

Fig. 5. Comparison between the SW curves resulting from simulations performed using a slowness and a slip evolution law (defined in Eqs. (1) and (2)) with the same constitutive parameters. The shape of the SW curves and the associated critical slip distance are very different: while the slowness law yields a nearly linear decay, the slip law yields a faster stress drop with variable weakening rate (τ).

duration of dynamic slip. Our numerical results show that the slip velocity peaks resulting for a slip law are much larger than those simulated for a slowness evolution law. This is consistent with the shorter critical slip weakening distance that in turns results in a faster fracture energy release (as evidenced by the larger weakening rate) and a smaller cohesive zone size. According to Perrin et al. (1995) and Zheng and Rice (1998), we find that a slip or a slowness law does not yield self-healing or short slip duration, but the resulting solutions are always consistent with a crack-like rupture mode. In particular, Perrin et al. (1995)

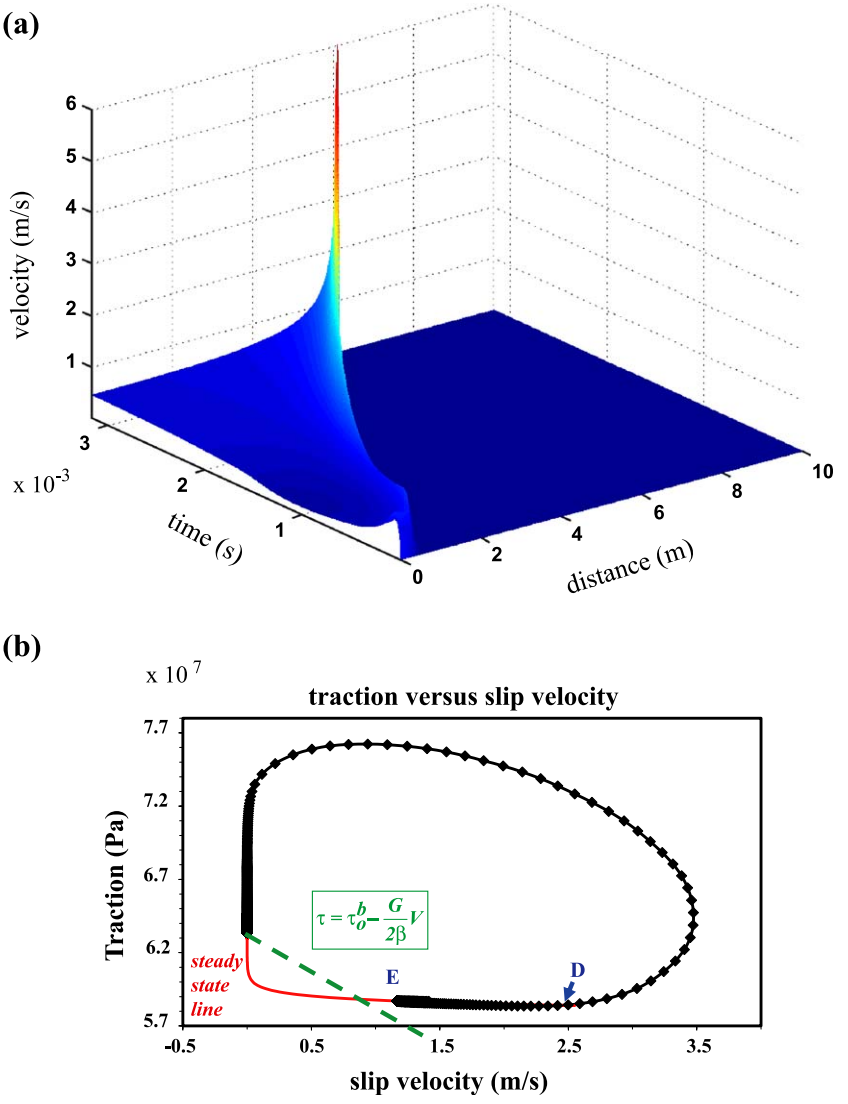

Fig. 6. Spatio-temporal evolution of slip velocity (a) for a crack obeying to the slowness evolution law for the same set of parameters as listed in Table 1 and used in Figs. 1–3. Slip velocity amplitudes increase during crack propagation but no healing appears. The phase diagram shown in the bottom panel (b) (same fault position as in previous figures) reveals that when the weakening phase is terminated (point D, see also Figs. 1 and 2), the dynamic evolution follows the steady state friction (D to E). The red curve in panel (b) indicates the steady state traction as a function of slip velocity, while the green one depicts the radiation damping line (see Zheng and Rice, 1998) defined by the equation included in the figure (G is the rigidity, β is the shear wave velocity and τ_0^b is the initial stress).

showed that no steady traveling pulse can occur if the constitutive law does not allow for restrengthening in truly stationary contact ($V=0$). Here we generalize the definition of self-healing pulses, also considering slip velocity time histories for which the residual velocity is very small although not necessarily zero after arrest. We have to remark that in a homogeneous fault self-healing pulses can be generated either by modifying the fault constitutive law or by imposing an impulsive mode during rupture initiation, which is self-maintained during the dynamic rupture propagation (see Nielsen and Madariaga, in press). We did not consider in this study the effect of stress and/or strength heterogeneity nor the effect of rupture propagation along a material interface. Our nucleation strategy does not prescribe the slip velocity pulse, because it is modeled as a time weakening controlled by the state variable (see Bizzarri et al., 2001 for further details). Fig. 6 shows the slip velocity dependence on time and space and the associated phase diagram: slip velocity does not return to zero and rupture healing does not occur. We remark again that while the slowness or slip evolution laws quantitatively describe the rupture initiation and propagation (see Lapusta and Rice, 2003) as well as the long-term restrengthening (see Rice, 1993; Boatwright and Cocco, 1996), they cannot generate a self-healing rupture propagation mode. Fig. 6 also shows that after the slip has reached its critical value for weakening (point D in the figure) the subsequent evolution follows the steady state friction (from D to E). We therefore confirm the results of Perrin et al. (1995) that a slowness and a slip law are unable to generate self-healing pulses.

5. The direct effect of friction

Beeler and Tullis (1996) have proposed two distinct strength functions that can yield fast restrengthening and self-healing following the Heaton (1990) suggestion that negative slip rate dependence can yield healing of slip. The first function is based on a sequential function characterized by a linear dependence on slip followed by a dependence on slip rate. Our simulations allow us to exclude this class of strength functions because we have shown that slip- and velocity-weakening occur simultaneously and not sequentially. The second function proposed by Beeler and Tullis (1996) is based on the rate- and state-dependent formulation, quite similar to that described by Eq. (1). They proposed a governing equation where the dependence on slip rate is eliminated by assuming a constant term for the direct effect of friction, which is included in the reference friction value (τ_{kf}):

$$\tau = \tau_{kf} + b\sigma_n \ln\Theta$$

$$\frac{d\Theta}{dt} = \frac{1}{L}\left[(V + V_{BT}) - \Theta V\right]$$

where V_{BT} is an arbitrary slip velocity value. In this formulation, the state variable is adimensional. Following Beeler and Tullis (1996), we investigate in this study the role played by the direct effect of friction and the friction behavior at high slip rates by using a slowness evolution law as defined in Eq. (1). Fig. 7 shows the time histories of slip, slip velocity, dynamic traction and state variable (a) and the spatio-temporal evolution of slip velocity (b) for two simulations having different values of the parameter a (0.009 and 0.0115, respectively) and leaving all the other parameters unchanged. This figure shows that the peak slip velocity increases when a decreases and the crack propagation is faster (in this case, the simulation with the smaller a even shows a crack bifurcation and a jump in rupture velocity). The traction drop is faster when the direct effect of friction is reduced (small a). This result is physically reasonable and both simulations show a crack-like rupture propagation mode. We point out that we were unable to generate self-healing using a slowness constitutive law also reducing the contribution of the direct effect of friction by changing the value adopted for the parameter a. We have also studied the effect of different velocity cutoff in the governing equation at high slip rates, depicted for the steady state friction in panel (a) of Fig. 8. We consider a governing equation, Eq. (1), in which friction depends on slip rate when $V \ll V_{cut}$, while for $V \gg V_{cut}$ the direct term is frozen and taken constant [a ln([V_*/V_{cut}]+1)]. In this case, friction still depends on slip velocity through the evolution equation and the state variable. We show in Fig. 8 the results of two simulations performed with two different values of the slip velocity cutoff (V_{cut}). The former calculations (shown in the left panels in Fig. 8) have a cutoff very close to the initial velocity (therefore, the direct effect of friction is constant and

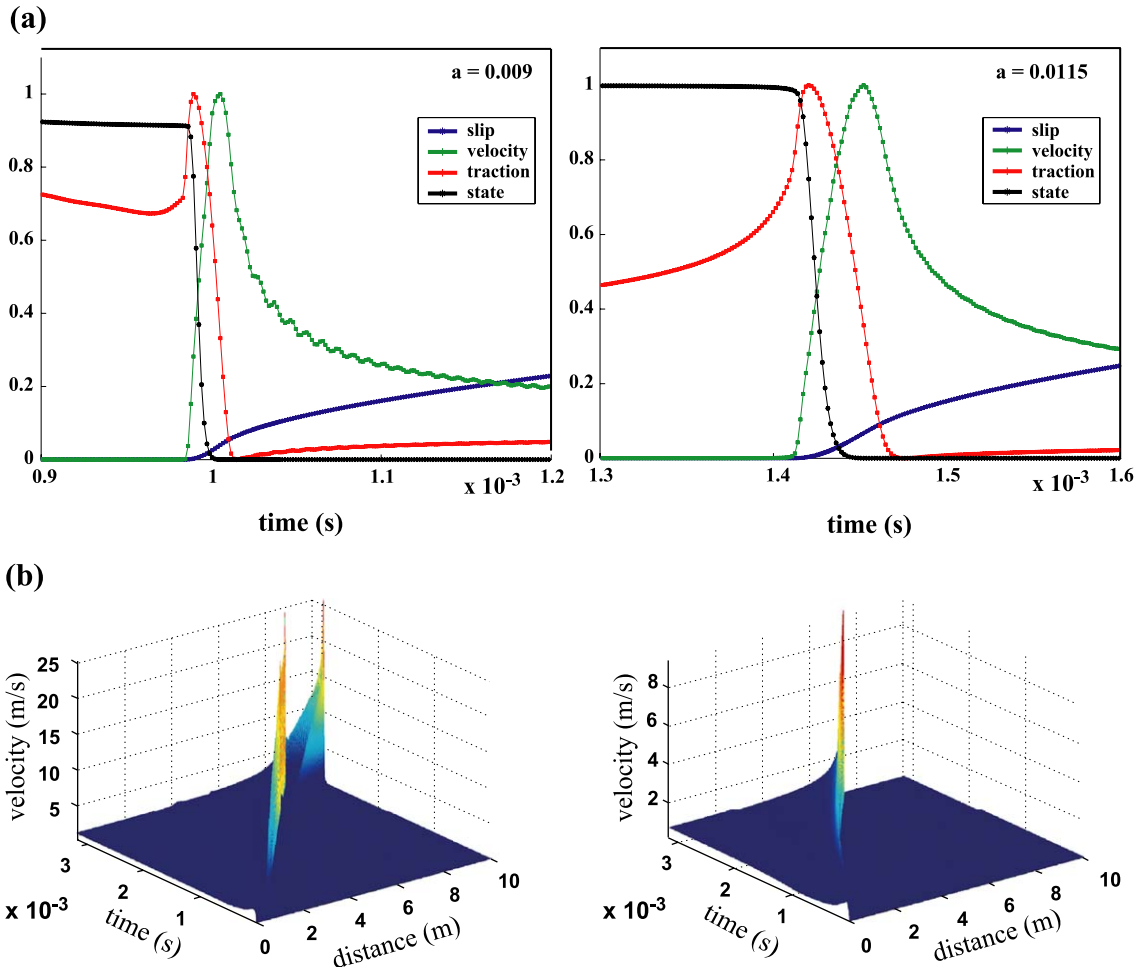

Fig. 7. Normalized time histories of relevant physical quantities (a) and spatio-temporal evolution of slip velocity (b) for two simulations performed with different values of the parameter a (all the other parameters are those listed in Table 1) controlling the direct effect of friction in the governing equation. A slowness evolution law is used for these calculations. Smaller values of the parameter a yield higher rupture velocities (the rupture front bifurcation occurs only in the simulation with the smaller value).

independent of slip rate during most of the simulation). The latter (right panels in Fig. 8) have a higher slip rate cutoff, so that the direct effect of friction is frozen only when $V>10^{-2}$ m/s. This figure shows that the direct effect of friction modifies the phase diagram reducing the velocity-hardening phase. In this case, the peak slip velocity occurs at the end of the weakening phase, when traction reaches the kinetic stress level and slip is equal to the critical distance (points C and D are now nearly coincident). When the velocity dependence of the direct effect of friction is eliminated, the phase diagrams display a nearly linear decay. On the contrary, if the slip rate controls the direct effect, the phase diagram is more elliptic and the velocity-hardening phase is more pronounced. We conclude however that in both cases we are unable to simulate self-healing pulse mode with a slowness evolution law.

It is important to point out that modifying the friction behavior at high slip rates affects the weakening processes within the cohesive zone. We show in Fig. 9 the slip weakening curves resulting from the simulations performed with different velocity cutoff and we compare them with the reference model shown in Fig. 1. This figure emphasizes that the direct effect

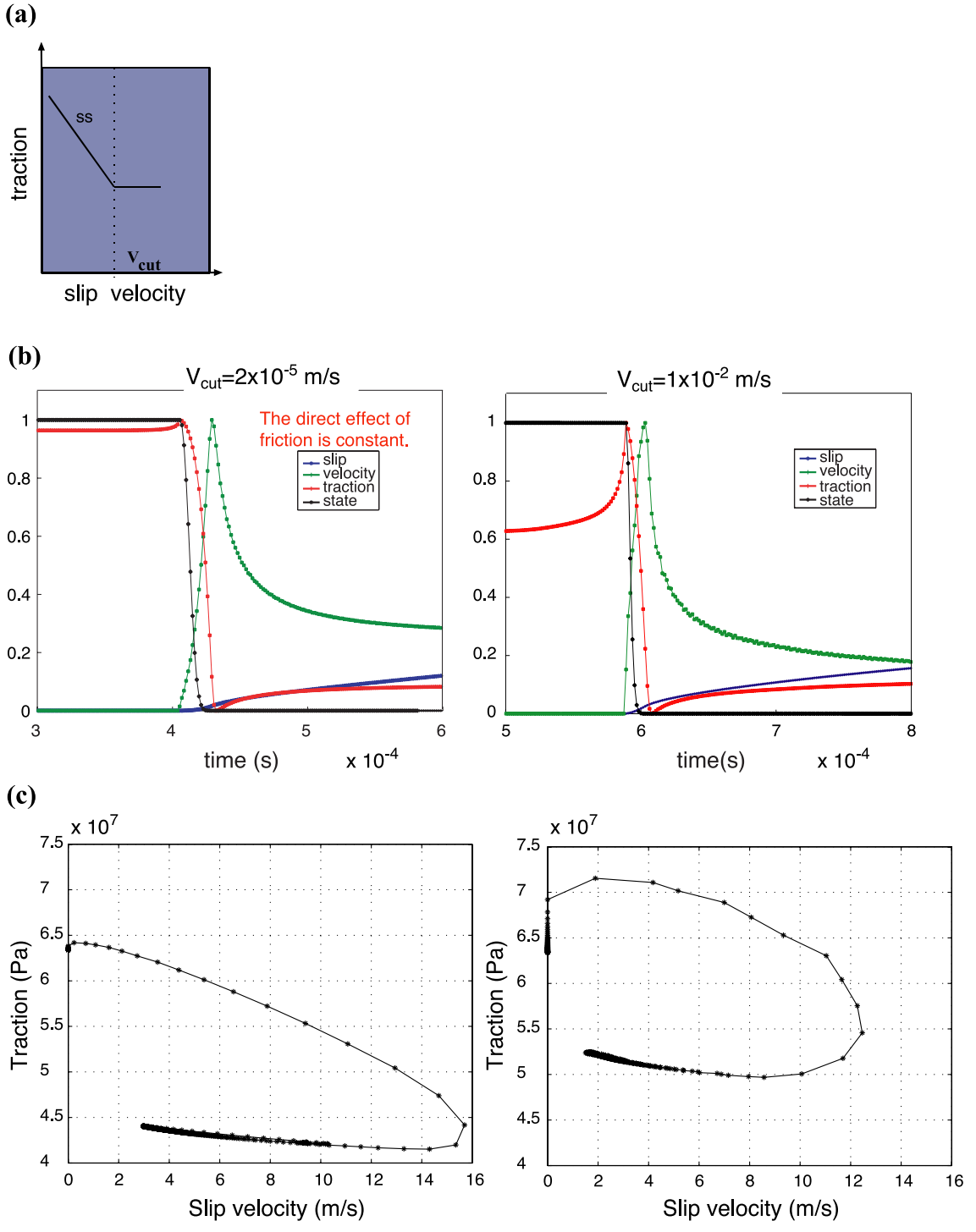
(a)
traction
ss
V_{cut}
slip velocity
(b)
V_{cut}=2x10^{-5} m/s
The direct effect of friction is constant.
slip
velocity
traction
state
time (s)
x 10^{-4}
V_{cut}=1x10^{-2} m/s
time(s)
(c)
x 10^{7}
Traction (Pa)
Slip velocity (m/s)

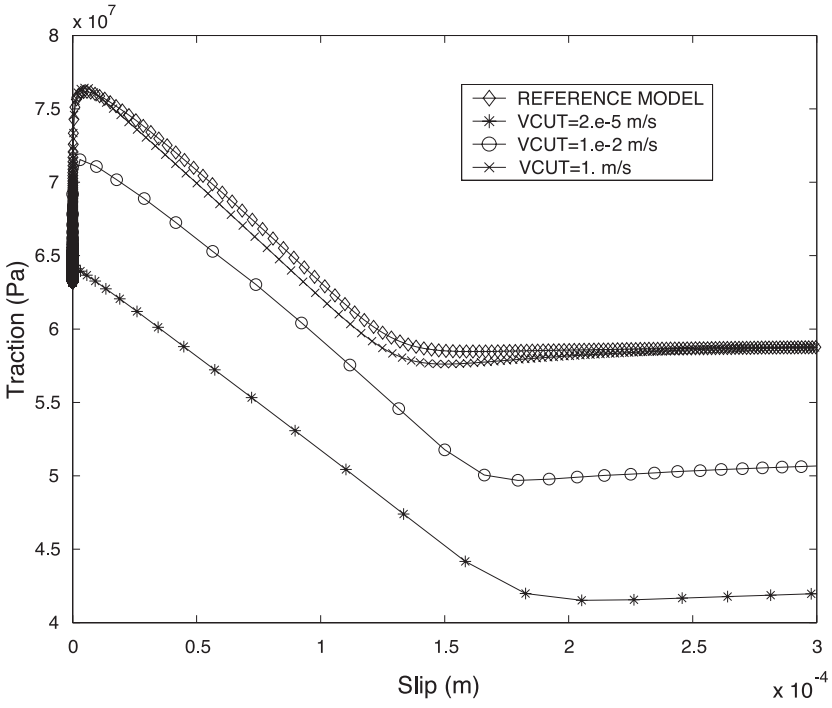

Fig. 9. SW curves calculated from several simulations performed using a slowness law and different values of the slip rate cutoff (V_{cut}). The SW curve shown in Fig. 1 is included for comparison, as the reference model.

of friction and the friction behavior at high slip rates largely control the kinetic stress level and the yield stress, while the equivalent slip weakening distance and the weakening rate are only slightly modified.

6. The evolution law and the healing mechanisms

We have discussed in the previous sections how the evolution law controls the dynamic rupture growth and the slip weakening behavior within the cohesive zone. We have also remarked that different modifications of the evolution law have been proposed to generate a self-healing or impulsive slip propagation mode. These attempts confirm our finding that the evolution law, peculiar of the rate and state formulation, plays a dominant role in controlling the breakdown process and the temporal and spatial evolution of dynamic traction and slip velocity. The motivation to modify the evolution law for modeling short slip duration or self-healing consists in the impossibility to have such behaviors using slowness or slip constitutive laws (defined in Eqs. (1) and (2)).

In this section, we present and discuss several simulations performed by using two other constitutive laws, which have been modified to have a fast restrengthening leading to the healing of slip. We start with the constitutive law proposed by Perrin et al. (1995) who suggested to modify the rate- and state-dependent laws used above to allow rapid restrengthening in truly stationary contact. These authors correctly emphasized that not all constitutive models allow

Fig. 8. Top panel (a) illustrates the adopted modification of friction behavior as a function of slip velocity for the steady-state traction. We assume that in the governing equation the direct effect of friction is constant and independent of slip velocity for $V>V_{cut}$, as explained in the text. (b) and (c) show the time histories of relevant physical quantities and the phase diagrams, respectively, calculated for two simulations performed using a slowness evolution law (1) with different values of V_{cut} (all the other parameters are those listed in Table 1). Left panels refer to a value which is only twice the initial velocity (the direct effect of friction is always independent of slip velocity during most of the simulation); while the right panels show the time histories and the phase diagram for a quite larger velocity cutoff.

for steady traveling wave pulses, and concluded that for the slowness and slip constitutive laws used above steady pulse solutions do not exist. We believe that the observational constraints for steady pulse or constant rise time during real earthquakes are quite weak. In this study, we attempt to model short rise times (that is, a slip duration much shorter than rupture duration which is independent of fault position) that are not expected with a crack-like rupture propagation mode. Perrin et al. (1995) proposed the following constitutive law:

$$\tau = \left[\mu* + a\ln\left(\frac{V+V_P}{V+V*}\right) + b\ln\left(\frac{\Theta(V*-V_P)}{L}+1\right)\right]\sigma_n^{\text{eff}},$$
$$\frac{d\Theta}{dt} = 1 - \frac{\Theta(V+V_P)}{L} \qquad (7)$$

where the velocity V_P represents a low velocity cutoff with no weakening at slip rates $V \ll V_P$ (see also Zheng and Rice, 1998). This version of the slowness evolution law allows for truly stationary contact ($V=0$) and gives an upper limit to a contact time $\Theta \le L/V_P$. Perrin et al. (1995) have shown that, using the constitutive law defined in Eq. (7), the spontaneous rupture propagation will occur either in the self-healing slip pulse mode (although not generally a steady pulse) or in the classical enlarging crack-like mode depending on the values of the adopted constitutive parameters. We show in Fig. 10 the spatio-temporal evolution of slip velocity simulated using our 2-D algorithm, the constitutive law defined in Eq. (7), and the set of constitutive parameters listed in Table 1 with $V*$ equal to 10 m/s and V_P equal to 10^{-2} m/s. This figure emphasizes that slip velocity becomes very small and healing of slip clearly occurs. Slip duration is short and it is not associated to a steady pulse traveling along the fault. Fig. 11 shows the time histories of state variable, slip, slip velocity and total dynamic traction and it points out again that the state variable drives the evolution of dynamic traction and the slip acceleration. The time window used in Fig. 11 is too short to show the total duration of slip, but this is required to compare the different time histories. However, the comparison between the time histories shown in this figure with those shown in Figs. 2 and 7 reveals the rapid increase of dynamic traction immediately after the end of the weakening phase, which is due to the fast restrengthening causing the healing of slip. This is even more evident in Fig. 12 where we have plotted the slip weakening curve and the phase diagram resulting from the constitutive law defined in Eq. (7). The dynamic traction shows an evident slip-hardening

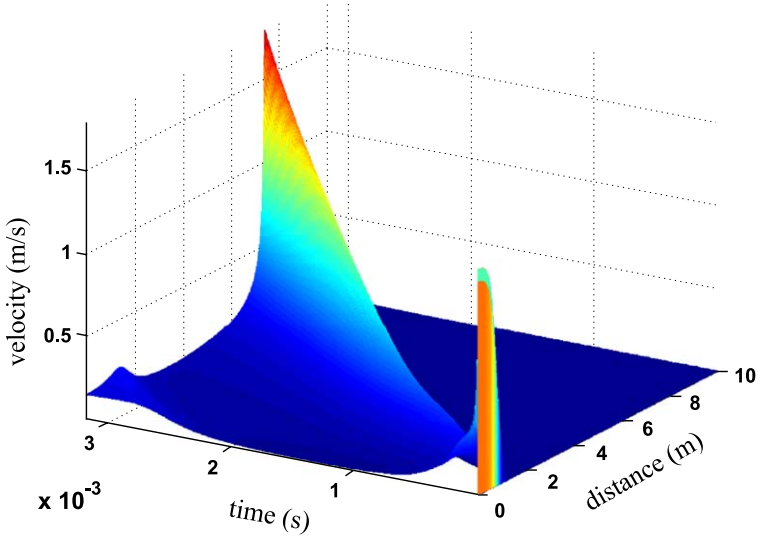

Fig. 10. Spatio-temporal evolution of slip velocity from a simulation performed using the constitutive law proposed by Perrin et al. (1995) and stated in Eq. (7). The nucleation patch is shown by the larger initial slip rate. The reference slip velocity $V*$ in this simulation is equal to 10 m/s and the low velocity cutoff V_P in Eq. (7) is 10^{-2} m/s. The solution shows healing of slip. The rapid restrengthening is so fast that the nucleation patch undergoes to an aseismic slip episode during the considered time window.

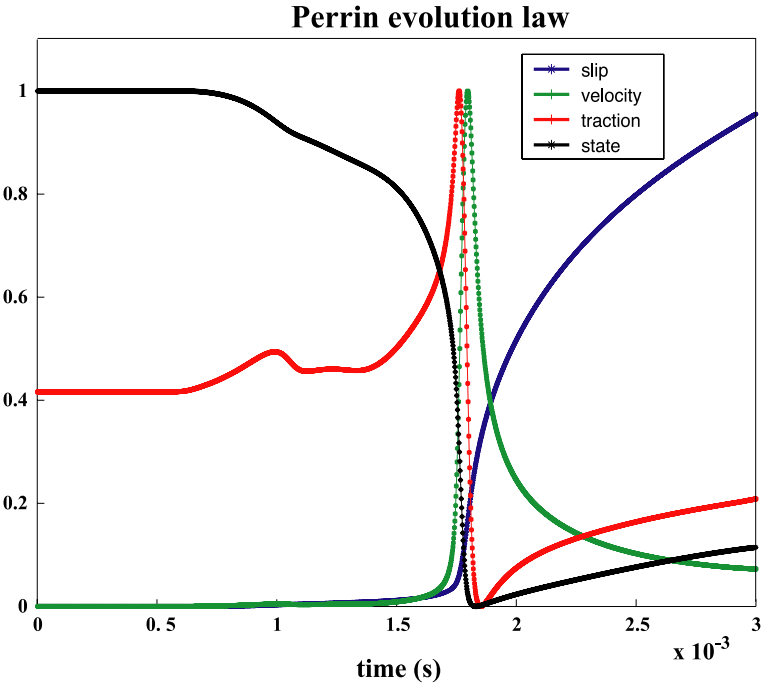

Fig. 11. Normalized time histories of slip, slip velocity, state variable and total dynamic traction calculated with the constitutive law described in Eq. (7).

phase preceding the slip weakening (which is in general more pronounced than that obtained with the constitutive models previously discussed) and the kinetic friction level is maintained only for a short time because the rapid restrengthening causes the dynamic traction increase. The phase diagram is also peculiar since the dynamic system, after an evident velocity hardening and weakening phases, does not follow the steady state friction, which means that the state variable is not constant or at the steady state. The rapid restrengthening is so fast that during the time window of the dynamic propagation the rupture re-nucleates, or re-accelerates if the arrest is not actually completed (see Fig. 10).

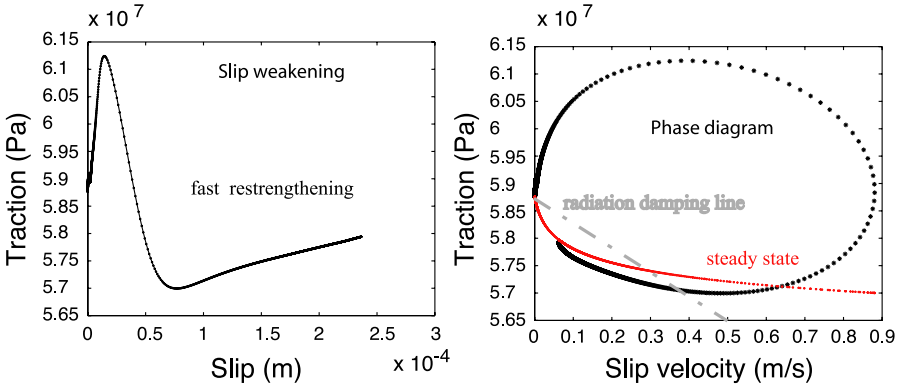

Fig. 12. SW curve and phase diagram resulting from the simulation performed with the constitutive law described in Eq. (7). The red curve shows the steady state friction as a function of slip velocity. The straight dot-dashed (grey) line represents the radiation damping curve (see Fig. 6 for comparison).

The constitutive law (Eq. (7)), proposed by Perrin et al. (1995), includes a modification of the slowness constitutive relation (Eq. (1)) motivated by the physical requirement to allow stationary contact. Many different modifications of the rate and state constitutive laws have been proposed in the literature to attempt to explain self-healing or other dynamic processes, but only few of them are based on physical requirements. Nielsen and Carlson (2000) proposed a state-dependent friction law that incorporates rate weakening and a characteristic time for healing. In this study, we have used a constitutive law where the governing equation is the same as the one used in Eq. (1) but the evolution law is that proposed by Nielsen et al. (2000) and Nielsen and Carlson (2000). This constitutive model has the form:

$$\begin{cases} \tau = \left[\mu_* - a\ln\left(\dfrac{V_*}{V}+1\right) + b\ln\left(\dfrac{\Phi V_*}{L}+1\right)\right]\sigma_n^{\mathrm{eff}} \\ \dfrac{\mathrm{d}}{\mathrm{d}t}\Phi = \dfrac{\gamma-\Phi}{t_{\mathrm{fh}}} - \dfrac{\Phi V}{L} \end{cases} \tag{8}$$

where γ has the dimensions of seconds and is taken equal to 1 and t_{fh} is the characteristic time for healing.

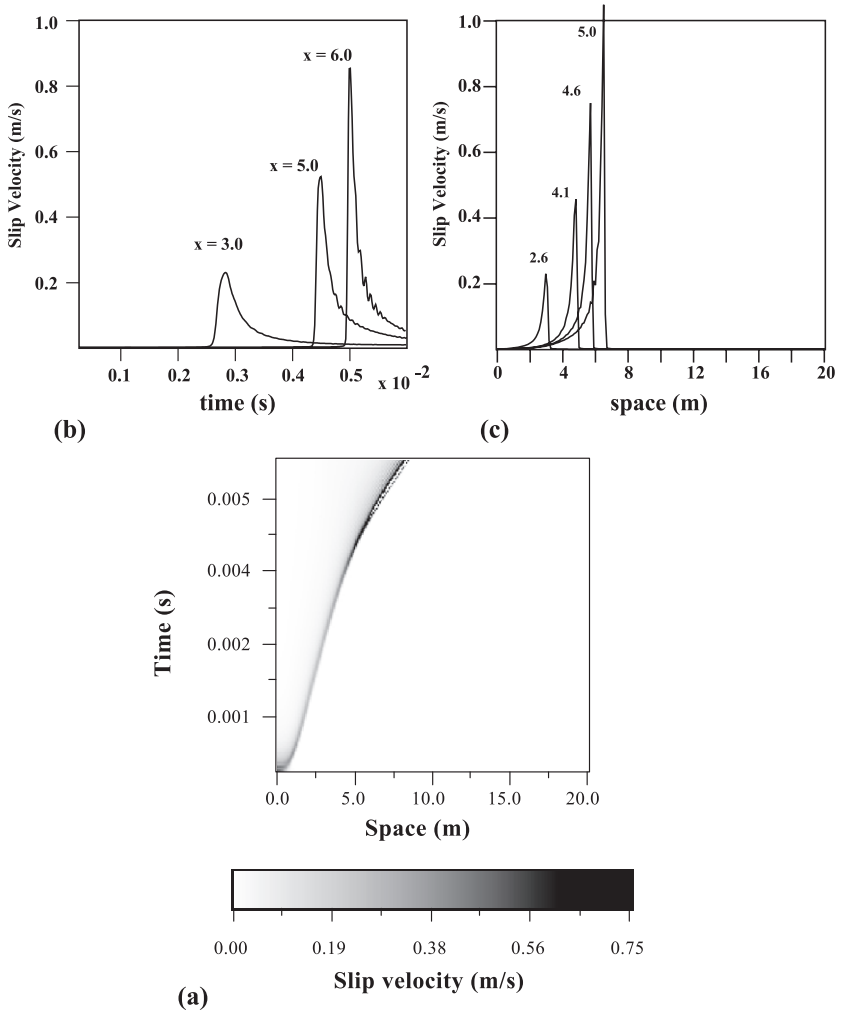

Fig. 13. (a) Spatio-temporal evolution of slip velocity calculated for a simulation performed using the constitutive law described in Eq. (8) and a characteristic values for t_{fh} equal to 3.9×10^{-3} s. The top panels show the slip velocity as a function of time (b) at different points on the fault line and of space (c) calculated at different time steps (in seconds).

The constitutive model described in Eq. (8) is different from that used by Nielsen and Carlson (2000) because we used a lab-derived governing equation in which we assign appropriate values to the parameters a and b. Moreover, we performed simulations with a dimensional data set that we will discuss in the following.

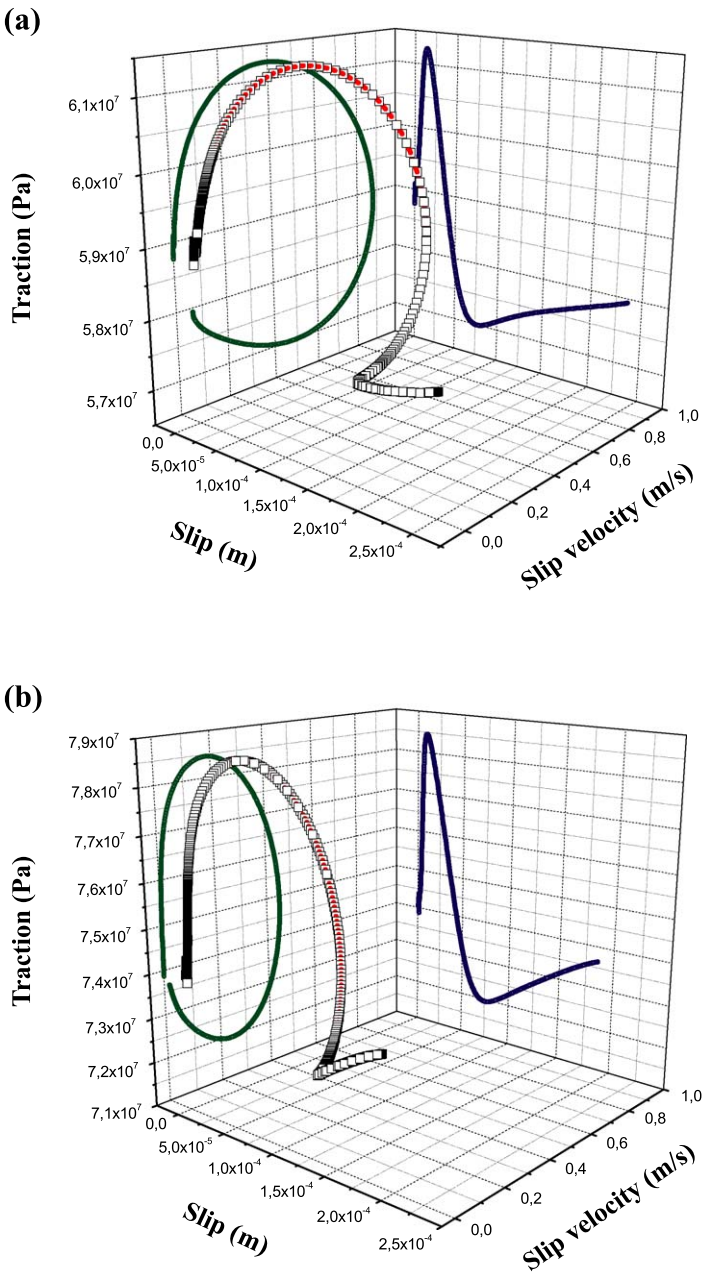

Fig. 14. Comparison between the 3-D phase trajectories resulting from the simulations performed with the constitutive laws described in Eq. (7) (top panel -a-) and Eq. (8) (bottom panel -b-) and showing total dynamic traction as a function of slip and slip velocity. The slip-weakening behavior resulting from these two distinct constitutive laws is very similar, while the inferred values of slip velocity are quite different.

We have performed several simulations using the constitutive model (8) with the same set of parameters used in previous figures (listed in Table 1) and changing the value of the characteristic time t_{fh}. Our simulations show that if the characteristic time is appropriately chosen, the solutions show a slip-pulse propagation mode with a nearly constant rise time. Values of the characteristic time larger than 0.1 s yield

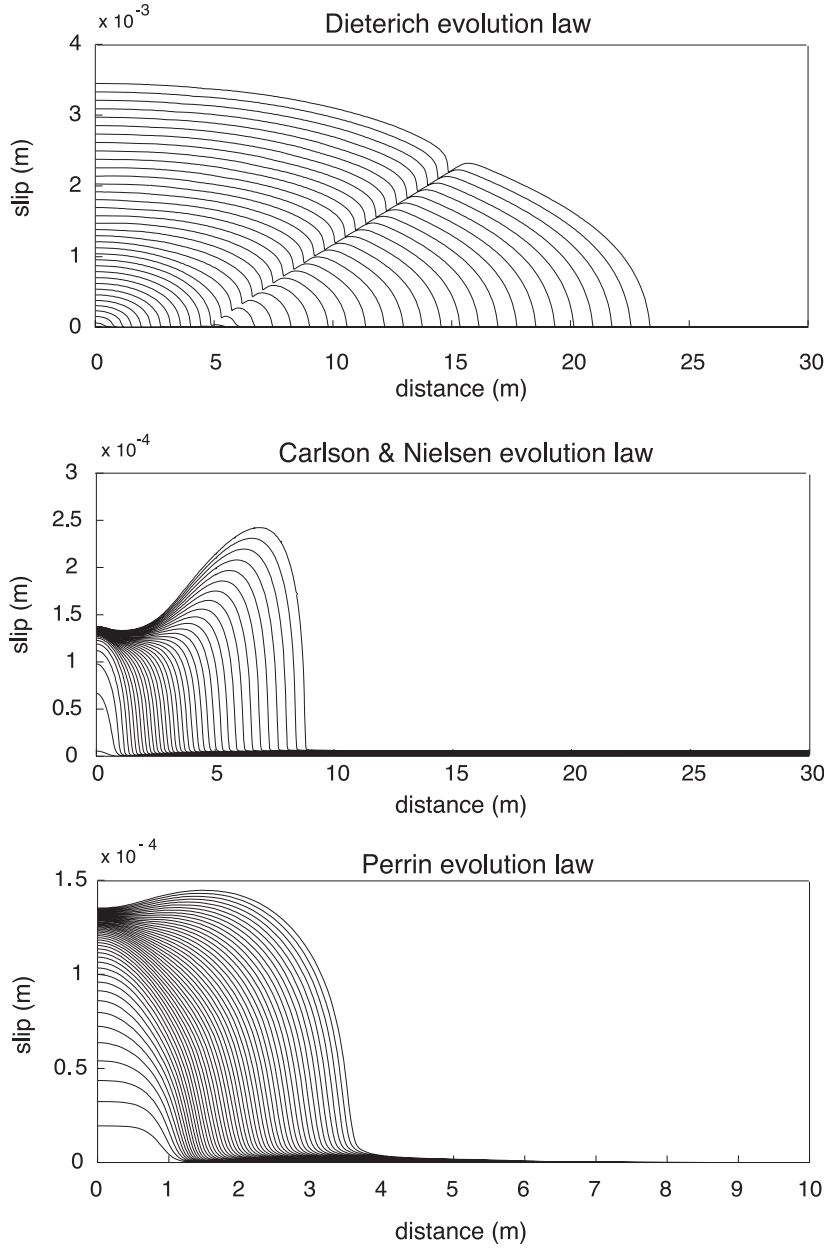

Fig. 15. Comparison between the slip profiles, obtained by the superposition of snapshots at different time steps of slip along the fault line, resulting from simulations performed with a slowness evolution law (top panel) and with the evolution laws described in Eq. (8), middle panel, and Eq. (7) bottom panel.

temporal evolution of slip velocity and dynamic traction very similar to the reference model shown in Figs. 1 and 2. The healing of slip occurs when t_{fh} becomes smaller than 5×10^{-3} s. Fig. 13 shows the results of a simulation performed using the values of parameters listed in Table 1 and a value of the characteristic time for healing (t_{fh}) of 3.9×10^{-3} s: slip velocity behavior shows a nearly constant duration and its peak increases as the crack advances. Fig. 14 shows a 3-D plot with the traction dependence on slip and slip velocity. This figure shows a phase diagram quite similar to those previously discussed and a rapid increase of dynamic traction (restrengthening) immediately following the slip weakening phase that generates the healing of slip. Fig. 14 shows a comparison between the 3-D phase trajectories resulting from the constitutive models (7) and (8) [a and b, respectively], which are very similar. The results of our simulations are summarized in Fig. 15 where we plot the superposition of slip profiles calculated at different times for three different constitutive models. The top panel shows the slip behavior resulting from the classical slowness law defined in Eq. (1) and it reveals that no healing occurs and the rupture propagates in the enlarging crack-like mode. The other two panels show the slip behavior resulting from the Nielsen and Carlson (2000) and the Perrin et al. (1995) constitutive models defined in Eqs. (8) and (7), respectively. These models show short slip durations resembling a self-healing propagation mode.

These results confirm that appropriate modifications of the evolution law can lead to self-healing slip propagation mode, but this requires the introduction of other characteristic parameters [a velocity cutoff in Eq. (7), or a characteristic time in Eq. (8)] that must be chosen without objective constraints. This implies that healing occurs with these constitutive laws only for particular set of the initial and constitutive parameters.

7. Discussions and conclusive remarks

In this paper, we aim to provide a physical interpretation of the breakdown process in order to explain the weakening mechanisms responsible for crack propagation and healing of slip. We model a 2-D in-plane rupture propagation along a homogenous fault line and we adopt rate- and state-dependent constitutive laws. We have demonstrated that this constitutive model allows the quantitative simulation of the rupture initiation and propagation and involves slip weakening within the cohesive zone. The critical distance of slip weakening is not the characteristic length scale parameter of the dynamic problem: In fact, in this formulation the parameter L for state evolution (renewal of the population of asperity contacts) is the characteristic length scale parameter. In agreement with Cocco and Bizzarri (2002), we find that these two parameters are different. We conclude that slip weakening is a characteristic feature of the dynamic failure episode characterizing the breakdown process, but the traction drop with increasing slip is controlled by the physical processes governing the constitutive behavior. Bizzarri and Cocco (2003) have demonstrated that the state variable evolution controls the slip-weakening behavior. We have extended this analysis to demonstrate that in the framework of rate and state constitutive laws the evolution equation of state variable governs both the weakening mechanisms and the healing of slip. We have compared different evolution laws and we conclude that slowness and slip constitutive models appropriately describe the rupture initiation and propagation but are unable to generate slip velocity pulses or short rise time, since the rupture grows as an enlarging crack-like mode. Therefore, the choice of the evolution law is crucial to represent the weakening and healing mechanisms in a homogeneous fault. We emphasize again that the slip weakening occurring within the cohesive zone is driven by the state variable evolution, which governs slip acceleration and deceleration (weakening and healing).

In order to perform the simulations discussed in this study and to interpret the state variable evolution it is necessary to have an optimal resolution of the cohesive zone. This implies that, even if the convergence and stability criteria are satisfied and solutions are found in a continuum model of fault dynamics, it is necessary to choose accurately the spatial and temporal discretization to follow and image the fast state variable evolution (see Bizzarri and Cocco, 2003, for further details and numerical tests). This observation explains the intrinsic limitation in constraining constitutive parameters and slip velocity evolution by modeling radiated seismic waves (see also Guatteri and Spudich, 2000), which would re-

quire the modeling of high frequency waveforms. Because the zone of very rapid state evolution (controlling stress and slip velocity behaviors at the crack tip) scales with L, estimating the value of this length scale parameter is crucial to define the resolution and to identify the dimensions of nucleation patch and cohesive zone. If for instance we use $L=2$ mm, which is large for numerical calculations but within the range of values estimated in laboratory experiments (see Mair and Marone, 1999), the nucleation patch is slightly less than 1 km but the cohesive zone is much smaller of the order of several tens of meters (≈ 60 m). This quantifies the fact that the spatial scales of our problems are very different. For these reasons, it is computationally expensive to perform 3-D simulations of a spontaneous rupture growth where the state variable is free to evolve according to the adopted constitutive model. Therefore, for these purposes, the adoption of a slip-weakening model is much more practical, because it allows us to prescribe the traction evolution within the cohesive zone, to constrain the fracture energy and to simulate radiated ground motions. As pointed out by Bizzarri and Cocco (2003), the dependence of SW parameters (see Eqs. (4)–(6)) on slip velocity values, which are unknown a priori, makes the simulation of spontaneous rupture propagation with rate and state constitutive models less feasible.

We have demonstrated in this study that, in the framework of a rate and state formulation, appropriate modifications of the evolution law allow us to simulate spontaneous ruptures propagating as a slip velocity pulse with short rise times, thus including self-healing. These constitutive models are characterized by a rapid restrengthening occurring immediately after the end of the weakening stage. However, these constitutive laws have never been tested to simulate the whole seismic cycle or the quasi-static earthquake nucleation. Therefore, we point out that the modeling of self-healing rupture mode, which implies a fast restrengthening, might not be appropriate to simulate the fault behavior during the interseismic period or the quasi-static nucleation. This raises the question on the reliability of these analytical modifications of lab-derived constitutive laws to explain short slip durations, even when motivated by physical arguments. Certainly, the ambitious perspective of dynamic modeling investigations is the simulation of fault behavior during the entire seismic cycle. This requires us to describe the earthquake nucleation, the dynamic rupture propagation and arrest during individual earthquakes (accurately describing the breakdown processes and the healing of slip) and the long-term restrengthening during the interseismic period, which yields to repeated dynamic failure episodes on the same fault. To this goal, it is important to look for a unified constitutive law describing most of these features. We have demonstrated that a rate and state formulation is able to provide a reliable physical description of individual earthquake ruptures, and we have discussed in this paper some of these features, but it also allows the modeling of repeated dynamic failure episodes. However, it has to be kept in mind that different competing natural mechanisms contribute to the understanding of earthquake mechanics. Physical models are very useful to separate their effects. By adopting the rate- and state-dependent laws, we try to incorporate the dependence of the friction coefficient on time as well as on the properties and roughness of the fault surface. However, other factors such as thermal pressurization and pore fluid lubrication (see Brodsky and Kanamori, 2001; Andrews, 2002) can affect the effective normal stress, thus modifying the friction law ($\tau=\mu\sigma_n^{\mathrm{eff}}$). Moreover, heterogeneities of constitutive parameters and complexities of fault geometry and earth structure should be considered in our modeling attempts. Short slip durations can be easily explained in terms of stress or strength heterogeneities (see Beroza and Mikumo, 1996; Bizzarri et al., 2001 among different others) or rupture propagation between dissimilar materials (Andrews and Ben-Zion, 1997; Cochard and Rice, 2000). These phenomena might explain short slip durations without modifying the constitutive law. Lapusta and Rice (2003) propose a similar reasoning to explain the earthquake nucleation and the early seismic propagation as well as the scaling of nucleation patch dimension with the size of the impending earthquake. Although appropriate modification of the evolution law allows the modeling of self-healing ruptures and the propagation of slip velocity pulses, we believe that heterogeneities of constitutive parameters and fault complexities can explain short slip durations without modifying the constitutive model.

Despite the existing limitations to assemble and to describe all the competing processes affecting earth-

quake mechanics, efforts to propose a unified constitutive law are very important to achieve a reliable physical description of the dynamic rupture growth. We believe that rate and state formulation is a suitable tool to this purpose, although further investigations and laboratory experiments are needed to explain the friction behavior at high slip rates or to include the effects of normal stress variations in the constitutive model (see Linker and Dieterich, 1992). The goal of our study is well below these tasks. We aim to identify and model those mechanisms occurring in the cohesive zone, which are controlled by the constitutive law. According to our results, we can interpret the breakdown process in terms of the roughness and the properties of the contact surface, which evolves during sliding. Thus, in this context, we extend the physical interpretation of the state variable evolution, proposed to describe the nucleation and the long-term restrengthening, to interpret the dynamic failure episode during the crack propagation (i.e., the breakdown process). The important conclusion of our study is that slip weakening should not be considered as an alternative description of the breakdown process. We propose that the state variable evolution controls slip weakening, because in the framework of a rate and state constitutive formulation it governs the weakening mechanisms and the slip acceleration. We have to remind here, however, that complementary interpretations of the state variable and its evolution law exist: Segall and Rice (1995) and Sleep (1997) proposed to relate the state variable to the porosity within the fault zone, thus accounting for the effects of dilatancy and pore compaction. Therefore, while we have shown that the evolution law governs the breakdown process, the physical interpretation of the state variable is not uniquely defined, because it depends on different competing mechanisms.

Acknowledgements

We thank Eiichi Fukuyama, Paul Spudich, Raul Madariaga and Stefan Nielsen for helpful discussions and criticism. We are indebted to Alain Cochard, Paul Spudich and an anonymous referee who reviewed the manuscript. We thank Joe Andrews for the positive feedback and the stimulating discussions on the numerical implementation of the algorithm. This research has been supported by INGV research funds of the Seismology and Tectonophysics department. We thank Enzo Boschi for his continuous encouragements and support to this research team.

References

Andrews, D.J., 1973. A numerical study of tectonic stress release by underground explosions. Bull. Seismol. Soc. Am. 63 (4), 1375–1391.

Andrews, D.J., 1976a. Rupture propagation with finite stress in antiplane strain. J. Geophys. Res. 81 (20), 3575–3582.

Andrews, D.J., 1976b. Rupture velocity of plane strain shear cracks. J. Geophys. Res. 81 (32), 5679–5687.

Andrews, D.J., 2002. A fault constitutive relation accounting for thermal pressurization of pore fluid. J. Geophys. Res. 107 (B12), 2363. (doi:10.1029/2002JB001942)

Andrews, D.J., Ben-Zion, Y., 1997. Wrinkle-like slip pulse on a fault between different materials. J. Geophys. Res. 102 (B1), 553–571.

Aochi, H., Fukuyama, E., 2002. Three-dimensional nonplanar simulation of the 1992 Landers earthquake. J. Geophys. Res. 107 (B2), 2035. (doi:10.1029/2000JB000061)

Barenblatt, G.I., 1959. The formation of brittle cracks during brittle fracture. General ideas and hypotheses. Axially-symmetric cracks. Appl. Math. Mech. 23, 1273–1282.

Beeler, N.M., Tullis, T.E., 1996. Self-healing slip pulses in dynamic rupture models due to velocity-dependent strength. Bull. Seismol. Soc. Am. 86 (4), 1130–1148.

Beeler, N.M., Tullis, T.E., Weeks, J.D., 1994. The roles of time and displacement in the evolution effect in rock friction. Geophys. Res. Lett. 21 (18), 1987–1990.

Beroza, G., Mikumo, T., 1996. Short slip duration in dynamic rupture in the presence of heterogeneous fault properties. J. Geophys. Res. 101, 22449–22460.

Bizzarri, A., Cocco, M., 2003. Slip-weakening behavior during the propagation of dynamic ruptures obeying to rate- and state-dependent friction laws. J. Geophys. Res. 108 (B8), 2373. (doi:10.1029/2002JB002198)

Bizzarri, A., Cocco, M., Andrews, D.J., Boschi, E., 2001. Solving the dynamic rupture problem with different numerical approaches and constitutive laws. Geophys. J. Int. 144, 656–678.

Boatwright, J., Cocco, M., 1996. Frictional constraints on crustal faulting. J. Geophys. Res. 101 (B6), 13895–13909.

Brodsky, E.E., Kanamori, H., 2001. Elastohydrodynamic lubrication of faults. J. Geophys. Res. 106, 16357–16374.

Cocco, M., Bizzarri, A., 2002. On the slip-weakening behavior of rate- and state-dependent constitutive laws. Geophys. Res. Lett. 29 (11), 1–4.

Cochard, A., Madariaga, R., 1994. Dynamic faulting under rate-dependent friction. Pure Appl. Geophys. 142, 419–445.

Cochard, A., Madariaga, R., 1996. Complexity of seismicity due to highly rate-dependent friction. J. Geophys. Res. 101, 25321–25336.

Cochard, A., Rice, J.R., 2000. Fault rupture between dissimilar

materials: ill-posedness, regularization, and slip pulse response. J. Geophys. Res. 105, 891–907.
Dieterich, J.H., 1979. Modeling of rock friction: 1. Experimental results and constitutive equations. J. Geophys. Res. 84, 2161–2168.
Dieterich, J.H., 1986. A model for the nucleation of earthquake slip. In: Das, S., Boatwright, J., Scholz, C.H. (Eds.). Earthquake Source Mechanics, Geophysical Monograph. 37. Maurice Ewing Series, 6, Am. Geophys. Union. Washington, DC, pp. 37–47.
Dieterich, J.H., 1992. Earthquake nucleation on faults with rate- and state-dependent strength. Tectonophysics 211, 115–134.
Dieterich, J.H., 1994. A constitutive law for rate of earthquake production and its application to earthquake clustering. J. Geophys. Res. 99, 2601–2618.
Dieterich, J.H., Kilgore, B., 1994. Direct observations of frictional contacts: new insights for state-dependent properties. Pure Appl. Geophys. 143, 283–302.
Gu, J.C., 1984. Frictional resistance to accelerating slip. Pure Appl. Geophys. 122, 662–679.
Gu, Y., Wong, T.F., 1991. Effects of loading velocity, stiffness, and inertia on the dynamics of a single degree of freedom spring slider system. J. Geophys. Res. 96, 21677–21691.
Guatteri, M., Spudich, P., 2000. What can strong-motion data tell us about slip-weakening fault-friction laws? Bull. Seismol. Soc. Am. 90 (1), 98–116.
Guatteri, M., Spudich, P., Beroza, G.C., 2001. Infering rate and state friction parameters from a rupture model of the 1995 Hyogo-ken Nambu (Kobe) Japan earthquake. J. Geophys. Res. 106, 26511–26521.
Heaton, T.H., 1990. Evidence for and implications of self-healing pulses of slip in earthquake rupture. Phys. Earth Planet. Inter. 64, 1–20.
Ida, Y., 1972. Cohesive force across the tip of a longitudinal-shear crack and Griffith's specific surface energy. J. Geophys. Res. 77, 3796–3805.
Ide, S., Takeo, M., 1997. Determination of constitutive relations of fault slip based on seismic wave analysis. J. Geophys. Res. 102 (B12), 27379–27391.
Lapusta, N., Rice, J.R., 2003. Nucleation and early seismic propagation of small and large events in a crustal earthquake model. J. Geophys. Res. 108 (B4), 2205. (doi:10.1029/2001JB000793)
Linker, M.F., Dieterich, J.H., 1992. Effects of variable normal stress on rock friction: observations and constitutive equations. J. Geophys. Res. 97, 4923–4940.
Mair, K., Marone, C.J., 1999. Friction of simulated fault gauge for a wide range of velocities and normal stresses. J. Geophys. Res. 104, 28899–28914.
Marone, C.J., 1998. Laboratory-derived friction laws and their application to seismic faulting. Annu. Rev. Earth Planet. Sci. 26, 643–696.
Marone, C.J., Kilgore, B., 1993. Scaling of the critical slip distance for seismic faulting with shear strain in fault zones. Nature 362, 618–621.
Nakatani, M., 2001. Conceptual and physical clarification of rate and state friction: frictional sliding as a thermally activated rheology. J. Geophys. Res. 106 (B7), 13347–13380.
Nielsen, S., Carlson, J.M., 2000. Rupture pulse characterization: self-healing, self-similar, expanding solutions in a continuum model of fault dynamics. Bull. Seismol. Soc. Am. 90, 1480–1497.
Nielsen, S., Madariaga, R., in press. On the self-healing fracture mode. Bull. Seismol. Soc. Am.
Nielsen, S., Carlson, J.M., Olsen, K.B., 2000. Influence of friction and fault geometry on earthquake rupture. J. Geophys. Res. 105, 6069–6088.
Ohnaka, M., 1996. Nonuniformity of the constitutive law parameters for shear rupture and quasistatic nucleation to dynamic rupture: a physical model of earthquake generation processes. Proc. Natl. Acad. Sci. U. S. A. 93, 3795–3802.
Ohnaka, M., Shen, L.F., 1999. Scaling of the shear rupture process from nucleation to dynamic propagation: implications of geometric irregularity of the rupturing surfaces. J. Geophys. Res. 104, 817–844.
Ohnaka, M., Yamashita, T., 1989. A cohesive zone model for dynamic shear faulting based on experimentally inferred constitutive relation and strong motion source parameters. J. Geophys. Res. 94, 4089–4104.
Okubo, P.G., 1989. Dynamic rupture modeling with laboratory-derived constitutive relations. J. Geophys. Res. 94 (B9), 12321–12335.
Okubo, P.G., Dieterich, J.H., 1984. Effects of physical fault properties on frictional instabilities produced on simulated faults. J. Geophys. Res. 89, 5817–5827.
Palmer, A.C., Rice, J.R., 1973. The growth of slip surfaces in the progressive failure of over-consolidated clay. Proc. R. Soc. Lond., Ser. A 332, 527–548.
Perrin, G., Rice, J.R., Zheng, G., 1995. Self-healing slip pulse on a frictional surface. J. Mech. Phys. Solids 43, 1461–1495.
Rice, J.R., 1993. Spatio-temporal complexity of slip on a fault. J. Geophys. Res. 98, 9885–9907.
Roy, M., Marone, C.J., 1996. Earthquake nucleation on model faults with rate- and state-dependent friction: effects of inertia. J. Geophys. Res. 101, 13919–13932.
Ruina, A.L., 1980. Friction laws and instabilities: a quasistatic analysis of some dry frictional behavior, PhD Thesis in Engineering at Brown University, Providence, RI.
Ruina, A.L., 1983. Slip instability and state variable friction laws. J. Geophys. Res. 88 (B12), 10359–10370.
Scholz, C.H., 2002. The Mechanics of Earthquake and Faulting, 2nd edition. Cambridge Univ. Press, Cambridge.
Segall, P., Rice, J.R., 1995. Dilatancy, compaction and slip instability on a fluid infiltrated fault. J. Geophys. Res. 100, 22155–22171.
Sleep, N.H., 1997. Application of a unified rate and state friction theory to the mechanics of a fault zones with strain locations. J. Geophys. Res. 102, 2875–2895.
Weertman, J., 1980. Unstable slippage across a fault that separates elastic media of different elastic constants. J. Geophys. Res. 85, 1455–1461.
Zheng, G., Rice, J.R., 1998. Conditions under which velocity-weakening friction allows a self-healing versus a crack like mode of rupture. Bull. Seismol. Soc. Am. 88, 1466–1483.